First posted online on 16 October 2020 as 10.1242/dmm.046383
Access the most recent version at http://dmm.biologists.org/lookup/doi/10.1242/dmm.046383

Alcoholic hepatitis and metabolic disturbance in female mice : a more tractable model than *Nrf2-/-* animals

Lozan Sheriff[#1], Reenam S. Khan[#1], Raquel Saborano[1], Richard Wilkin[1], Nguyet-Thin Luu[1], Ulrich L.Gunther[2], Stefan G. Hubscher[1,3], Philip N. Newsome[1], Patricia F. Lalor[1]

[1]Centre for Liver and Gastroenterology Research and Birmingham National Institute for Health Research (NIHR) Birmingham Biomedical Research Centre, Institute of Immunology and Immunotherapy, University of Birmingham, Birmingham, UK. [2]Institute of Cancer and Genomic Sciences, University of Birmingham, and Institute of Chemistry and Metabolomics, University of Lübeck, Lübeck Germany. [3]Liver Unit, University Hospitals Birmingham, Birmingham, UK; Institute of Immunology and Immunotherapy, University of Birmingham, UK; Dept. of Cellular Pathology, University Hospitals Birmingham, UK.

Corresponding Author : Dr Patricia Lalor. p.f.lalor@bham.ac.uk Tel +44 121 4146967.

Address as above.

Keywords : Alcoholic hepatitis, inflammation, fibrogenesis, steatosis, murine

Declaration

This study includes independent research supported by the Birmingham National Institute for Health Research (NIHR) Birmingham Biomedical Research Centre based at the University of Birmingham. The views expressed are those of the authors and not necessarily those of the NHS, the National Institute of Health Research or the Department of Health and Social Science. RK was supported by a 2017 BSG-Guts UK Trainee Research Award. LS was supported by a Confidence in Concept grant from the Medical Research Council (MR-S001581) and an MRC Stratified Medicine Consortium fund : MICA: Minimising Mortality from Alcoholic Hepatitis (MR/R014019/1)

# These authors contributed equally to this work.

The authors have no competing interests to declare.

Abstract

Alcoholic hepatitis (AH) is the dramatic acute presentation of alcoholic liver disease, with a 28-day mortality of 15% in severe cases. Research into AH has been hampered by the lack of effective and reproducible murine models that can be operated under different regulatory frameworks internationally. The liquid Lieber-deCarli (LdC) diet has been used as a means of ad libitum delivery of alcohol, but without an additional insult, it is associated with relatively mild liver injury. The transcription factor Nuclear factor-erythroid 2-related factor 2 (*Nrf2*) protects against oxidative stress and mice deficient in this molecule are suggested to be more sensitive to alcohol-induced injury. We have established a novel model of AH in mice and compared the nature of liver injury in C57/BL6 wild type versus $Nrf2^{-/-}$ mice. Our data show that both WT and *Nrf2*-/- mice demonstrate a robust weight loss, increase in serum transaminase, steatosis and hepatic inflammation when exposed to diet and ethanol. This is accompanied by an increase in peripheral blood and hepatic myeloid cell populations, fibrogenic response and compensatory hepatocyte regeneration. We also noted characteristic disturbances in hepatic carbohydrate and lipid metabolism. Importantly use of *Nrf2*-/- mice did not increase hepatic injury responses in our hands and female wild type mice exhibited a more reproducible response. Thus, we have demonstrated that this simple murine model of AH can be used to induce an injury that recreates many of the key human features of alcoholic hepatitis, without the need for challenging surgical procedures to administer ethanol. This will be valuable for understanding of the pathogenesis of AH, for testing new therapeutic treatments or devising metabolic approaches to manage patients whilst under medical care.

INTRODUCTION

Alcoholic liver disease (ALD) places an enormous burden on patients, their carers and society as a whole. In the last 30 years, mortality from ALD has risen by 450%(AoM., 2004), and in part this relates to the more dramatic, acute form of disease, alcoholic hepatitis (AH). There is no approved therapy for AH and whilst drugs, including immune modulators and monoclonal antibodies have been tested for management of severe AH, only glucocorticoids and pentoxyfylline have been licensed for use(European Association for the Study of, 2012). However, two meta-analyses of pentoxyfylline use did not show convincing benefit (Louvet et al., 2018; Thursz et al., 2015). Similarly whilst the large randomised, controlled STOPAH trial showed that corticosteroids can improve short-term survival (28 days) in patients with severe AH, 40% of patients were considered 'non-responders' (Mathurin, 2005). Furthermore, no significant mortality benefit was seen with steroids at 90 days or one year in the STOPAH trial (Thursz et al., 2015). Importantly steroids have significant side effects including infection(Hmoud et al., 2016), sepsis, haemorrhage and hepato-renal syndrome. Therefore, the UK NIHR James Lind Alliance has identified AH as a priority translational research area due to lack of licensed therapies.

Research into new therapies for AH has been disadvantaged by the lack of effective murine models that recreate the features of human disease whilst being reproducible and acceptable to local regulatory policies. The pathogenesis of AH is multifactorial, and characterised by macrovesicular steatosis, infiltration of immune cells, and hepatocellular damage accompanied by an increase in serum transaminases. The inflammatory response is associated with impaired hepatocyte regeneration in response to injury. Additional histological changes include perivenular and pericellular fibrosis. Whilst a number of rodent models have been used to study AH, all have their individual challenges and deficiencies. Chronic ad libitum EtOH feeding using a Lieber–DeCarli (LdC) liquid diet has been widely tested, but generates a relatively mild injury without fibrosis when used alone(Han et al., 2013; Hu et al., 2013; Kirpich et al., 2012; Li et al., 2014; Zhang and Meadows, 2008). A number of two-hit models have attempted to generate more severe injury, by combining LdC

diet administration with use of genetically modified mice (Ji et al., 2006; Ji et al., 2004; Ki et al., 2010; Ronis et al., 2015), alcohol gavage (Chang et al., 2015; Lazaro et al., 2015), and lipopolysaccharide (LPS)(Kong et al., 2017; Wieser et al., 2017) for example. The National Institute on Alcohol Abuse and Alcoholism (NIAAA) developed a model of AH which involves chronic EtOH feeding in a high fat Lieber deCarli (LdC diet), followed by a single large binge of EtOH by gavage(Bertola et al., 2013b). This model does induce a robust neutrophil-mediated liver injury, but the high-dose ethanol binge causes mice to become moribund, which is not acceptable within all regulatory systems internationally. Similarly models involving continuous intragastric EtOH infusion(Tsukamoto et al., 1985a) are associated with severe hepatic steatohepatitis and mild fibrosis, but complex surgery, single-mouse housing and intensive monitoring are beyond remit for many facilities and not amenable to regulatory drug screening.

Thus simpler, less challenging models that recreate hepatic and systemic features of human AH are required for widespread utility. One option is to incorporate enhanced hepatic oxidative stress to generate a more significant injury than that generated by ethanol administration alone. In this context, the Nuclear factor-erythroid 2-related factor 2 (*Nrf2*) deficient mouse has been investigated. *Nrf2* is s transcription factor considered the 'master regulator' of anti-oxidant defences. Lamle *et al.,* (2008) suggested that *Nrf2* knockout mice (*Nrf2*$^{-/-}$) developed a more severe hepatic injury than wild-type (WT) mice given high dose gavage(Lamle et al., 2008). Thus we have adapted this model and describe a reproducible protocol that causes robust steatosis, elevation in serum transaminase levels and hepatic inflammation. However using this dietary protocol, we also show that use of *Nrf2*$^{-/-}$ deficient mice offers no advantage over female WT animals in our hands. Importantly we report systemic responses (weight loss, neutrophilia) and hepatic metabolic changes(Brandl et al., 2018; Ding et al., 2019; Latchoumycandane et al., 2014) (elevated taurine, lipid intermediates and lactate) as well as characteristic histological features (steatosis, and neutrophil infiltration) that provide insight into the steatogenic mechanisms that characterise

AH. Thus, in conclusion we would suggest that administration of a modified LdC diet to female WT mice represents a tractable and simple model of alcoholic hepatitis when combined with daily ethanol gavage.

METHODS

LdC diet and ethanol feeding.

All mice were maintained and housed under conventional conditions in the Biomedical Services Unit at the University of Birmingham, UK. All animal experiments were performed under a Home Office project license in accordance with UK legislation, and studies were approved by the local ethical review board. Specific pathogen free female 8-10 week old WT and *Nrf2*$^{-/-}$ mice on a *C57/BL6J* background, were obtained from the Charles Rivers Laboratories (Margate, U.K.; https://guide.labanimal.com/supplier/charles- river-uk-ltd). Female WT and *Nrf2*$^{-/-}$ mice were fed LdC liquid diet (Special Diet Services, UK) ad libitum for 5 days via specialised feeding tubes (Richter tubes). Preparation of the diet involved using a hand-held blender to mix a set volume of dry mix with maltose dextrin and water (See Table 1).

For experimental groups LdC diet was supplemented with escalating doses of ethanol (Alcohol : 95% proof ethanol, William Hodgson and Company, UK) over the following week (2.1% ethanol on day 7 increased to 4.2% at day 9, and 6.2% at day 12). All experimental mice were additionally gavaged twice daily with 33% of EtOH diluted with water from day 6 until day 15. Prior to gavage we completed a mouse physiological condition assessment sheet and the volume administered to healthy animals was determined by weight (190ul for mice 19g, 200µl for mice 20g, 250µl for mice >25g). Control mice were fed LdC diet without EtOH throughout the experiment with the amount of maltodextrin adjusted to maintain total calorie load in both groups (see Table 1). Blood and liver tissue were collected at the end of the experiment. Alanine aminotransferase (ALT), aspartate aminotransferase (AST), alkaline phosphatase (ALP) and bilirubin levels in murine serum as well as full blood count and differential were determined utilising clinical grade automated analysers at Birmingham Women's Hospital NHS Foundation Trust, Birmingham, UK.

Flow cytometry

Liver infiltrating immune cells were isolated from freshly harvested liver lobes. The liver was flushed with PBS before isolation to remove blood cells. The tissue was weighed and manually digested using a 70µm strainer (Falcon). The filtrate was diluted in cold RPMI and centrifuged twice at 700xg for 5 minutes. A working dilution of Optiprep (Sigma) at 1.09g/ml was obtained by mixing neat Optiprep with PBS at a 4:11 ratio. 5 ml of cell suspension was layered carefully over 7 ml of Optiprep solution, and centrifuged at 1000xg for 25 minutes. The mononuclear cells at the interface were washed twice and resuspended in PBS + 1% fetal calf serum. Cells were stained for 30 minutes in the dark with zombie (APC-Cy7 in a 1:1000 concentration) to assess live/dead status of cells. Samples were washed and incubated for 20 minutes with purified anti-mouse CD16/32 antibody (ebioscience, clone 93, 1:25 dilution of manufacturers stock) to block non-specific Fc- receptor binding. Finally, cells were incubated for 30 minutes with lineage specific antibodies for identification of myeloid and lymphoid cells (see Table 2).

Immunohistochemistry and histological analysis

Haematoxylin and eosin staining was performed on Formalin fixed, paraffin embedded sections from each mouse liver using standard protocols. Sections were reviewed by an experienced liver pathologist (SGH), blinded to the experimental conditions. For each case the pattern (large or small droplet), zonal distribution and severity of steatosis were recorded. Disease severity was scored semi-quantitatively for the overall degree of steatosis (0-3), the amount of large droplet steatosis (0-3), and the severity of inflammation according to the Kleiner system(Kleiner et al., 2005). For antibody staining, FFPE sections were deparaffinised with xylene and then rehydrated through graded alcohol prior to high-temperature antigen retrieval in pre-heated EDTA buffer (pH 8) for 15 minutes. Endogenous peroxidase activity was blocked (Dako-Peroxidase, Dako Ltd, Cambridge UK) for 10 minutes, and non-specific binding of the antibodies to the sections was prevented by incubation with X10 casein (Vector Labs Inc Burlingame, CA, USA) diluted in PBS. Sections

were incubated in primary antibody, or an isotype matched control for 1 hour at room temperature in a humidified chamber on a rocker. They were then washed twice, followed by addition of the relevant horse-radish peroxidase conjugated secondary antibody for 30 minutes and signal development using ImmPACT DAB reagent (Vector Labs). Sections were washed, counterstained with Mayer's haematoxylin, dehydrated with 99% alcohol, cleared with xylene and then mounted in DPX (Leica GmBH). The exact conditions were optimised for each antibody (see Table 3).

For image analysis, at least 5 fields of view were taken per sample using Brightfield microscopy with AxioScanner software at x20 magnification. The images were reviewed on Image J software version 1.42 (NIH). For Ki-67 staining, the number of positively staining hepatocytes per field was counted. For Ly6G staining, the number of positively staining cells was counted. For CD45 and F4/80 staining, morphometric analysis was performed.

Picrosirius Red and Oil red O staining

Deparaffinized, hydrated sections were placed into 5% phosphomolybdic acid solution (diluted in distilled water) for 5 min. Sections were washed with PBS and submerged in 0.1% Sirius red (Direct Red 80 dissolved in saturated picric acid solution) for 90 minutes on a rocker. The slides were dipped in acidified water (0.5% glacial acetic acid) for 30 seconds twice, followed by 100% ethanol three times for 30 seconds each. Finally staining intensity was determined using morphometric analysis via Image J software version 1.42 (NIH), using 5 non-overlapping fields selected at random from each mouse (at x20 magnification). To quantify lipid content in hepatocytes, fresh frozen tissue sections were incubated in 60% isopropanol for 5minutes followed by Oil Red O reagent for 15 minutes at room temperature. This was tipped off and 60% isopropanol was added for another 5 minutes. Slides were washed twice with water and finally mounted using aqueous mountant (Thermoscientific, Shandon). Sections were imaged using brightfield microscopy and % staining area was determined using morphometric analysis via Image J software version 1.42 (NIH), using 5 non-overlapping fields selected at random from each mouse (at x20 magnification).

Assessment of liver metabolism by NMR

Single lobes from mouse livers were collected at day 13,15 and 17 for mice exposed to LdC plus alcohol feeding. Matched livers from mice fed control LdC diet alone were collected on day 17. Tissue was immediately snap frozen upon collection and stored at -80°C until processing. To prepare extracts for NMR analysis, approximately 100 mg liver tissue was added to gentleMACs M-Tube in cold methanol (8 µL/mg) and purified water (2 µL/mg). Samples were homogenised using a gentleMACs homogenizer (Miltenyi, UK) and polar metabolites were extracted as described previously(Schofield et al., 2017) Samples were kept at 4°C prior to NMR. All spectra were acquired at 300 K on a Bruker 600 MHz spectrometer with a TCI 1.7mm z-PFG cryogenic probe using a cooled Bruker SampleJet autosampler as previously described (Saborano et al., 2019).1D ^{1}H NMR spectra were processed using the NMRlab and Metabolab programmes within MATLAB (MathWorks, Massachusetts, USA). Following Fourier transformation, spectra were phased, referenced to TMSP δ 0.00 ppm, baseline corrected and the water region was excluded together with the edges of the spectrum void of signal. Lastly, spectra were scaled to the total spectral area and resonances were assigned using Chenomx (Alberta, Canada, 2015), and by consulting the NMR metabolic profiling human metabolome database (HMDB). Further details can be found in(Saborano et al., 2019).

RESULTS

Exposure of WT and *Nrf2*$^{-/-}$ mice to LdC diet and ethanol causes inflammation and hepatic steatosis with early fibrogenic change

In order to induce a reproducible alcohol injury in mice, we modified a Lieber deCarli diet(Preedy et al., 1988; Wilkin et al., 2016) feeding protocol. Female WT and *Nrf2*$^{-/-}$ mice were fed liquid LdC diet alone for 5 days to acclimatize prior to addition of escalating doses of ethanol into the diet (up to a final concentration of 6.2% at day 12). Additional twice daily gavage with 33% of EtOH diluted with water was added from day 6 until day 15. Control

mice were fed LdC diet alone throughout the experiment. Whilst mean weight of the experimental and control groups was similar at baseline, both WT and *Nrf2*$^{-/-}$ mice lost a significant amount of weight after introduction of EtOH, with weight-loss approaching 20% by day 15 (Fig 1A). At day 15, both WT mice and *Nrf2*$^{-/-}$ exposed to LdC diet with EtOH showed significantly increased serum ALT levels compared to mice receiving LdC only, or normal chow (Fig 1B). Of note, AST levels were also significantly increased in *Nrf2*$^{-/-}$ mice receiving ethanol (Supp Fig 1). The AST:ALT ratio was >1, (mean AST: mean ALT was 1.63: 1 for WT mice and 2.53:1 for *Nrf2*$^{-/-}$ mice), but bilirubin levels were not significantly different between the groups (data not shown). Liver sections were scored for steatosis and inflammatory activity. Representative images in Figure 1A show that high fat diet alone had no effect on the histological changes seen in the livers of either WT or *Nrf2*$^{-/-}$ mice over the course of 15 days. We did note that for the *Nrf2*$^{-/-}$ animals, we observed occasional fields of view where there was a focus of inflammatory cells or areas of macrovesicular steatosis in animals fed LdC alone. However, this was variable between individuals and indeed between different fields of view on an individual liver section, and was not significant when multiple fields of view were scored (Figure 1C and D). However, the addition of ethanol caused a marked degree of steatosis which frequently included a mixture of large and small droplets. Amongst, the alcohol-treated mice, the distribution of large droplet fat within hepatocytes was variable but steatosis overall was predominantly centrilobular in location. Semi quantitative scoring (Fig1C) shows the magnitude of this response. This analysis was confirmed using Oil red O staining (Supplemental Figure 2). As before, a mixed micro and macrovesicular steatosis was evident in mice (both WT and *Nrf2*$^{-/-}$) exposed to ethanol plus diet, which was significantly above the background staining observed in livers from mice exposed to diet or chow alone. Image quantitation confirmed that steatosis was significantly greater in the presence of alcohol and diet feeding, and that both WT and *Nrf2*$^{-/-}$ mice showed a similar extent of steatosis. Importantly we did not observe hepatocyte ballooning or the presence of Mallory-Denk(Denk et al., 1979; Denk et al., 2000) bodies in any of the samples. Finally whilst there was evidence of focal inflammation in some animals, total inflammation scores were not significantly different between the groups (Fig 1D). In addition, in the groups of mice receiving ethanol, occasional mice demonstrated patches of necrosis on histological assessment.

Our observations of histological sections from our injured livers (Figure 1A) suggested that there was a trend for increased inflammatory response induced by ethanol exposure, particularly in WT animals. Analysis of full blood counts (Figure 2A) showed a significant increase in the proportion of neutrophils and monocytes in circulating blood in both WT and Nrf2-/- mice when ethanol was superimposed on LdC diet. This was accompanied by a

proportional decrease in circulating lymphocytes. Thus we next performed a cytometric analysis of liver resident immune cell populations as previously described(Weston et al., 2015) and stained for the presence of cells within liver tissue samples. In comparison to mice fed LdC alone, both WT and *Nrf2-/-* mice had a significantly greater proportion of CD11b+ cells within the liver after alcohol exposure. When we used F4/80 and Ly6G staining to discriminate between neutrophils and macrophages, we observed a significant increase in Ly6G+ cell recruitment to the liver after ethanol treatment, particularly in WT animals. These cells were distributed throughout the parenchyma (see images in Figure 2B). We used cytometric analysis to quantify hepatic myeloid cells (defined by live gating and then CD45+CD3-CD11b+as a percentage of total CD45+ cells) and hepatic neutrophils (defined by live gating and then CD45+CD3-F4/80-Ly6G+ as a percentage of total CD11b+ cells) for WT and *Nrf2-/-* mice. Hence we observed that the numbers of hepatic CD11b+ neutrophils significantly increased after exposure LdC plus ethanol. In contrast numbers of F4/80 positive macrophages/Kupffer cells and their hepatic distribution was unchanged by exposure to diet plus ethanol on immunohistochemical quantification (see Figure 2 and quantification of staining in Supplementary Figure 3).

Picrosirius red staining of liver sections (Figure 3) also indicated that there was a modest but significant accumulation of collagen in mice fed ethanol plus high fat diet at day 15, compared to diet alone. This was evidenced by the accumulation of stained collagenous fibrils in both the periportal areas and within the parenchyma of alcohol exposed animals. Whilst the short duration of our model meant that the extent of staining was modest indicative of a very early fibrogenic activation (see images in Figure 3B), it was interesting to note that *Nrf2*$^{-/-}$ mice were more variable in response, and only WT mice showed a significant difference between LdC diet alone, and diet plus ethanol (Fig 3A).

LdC diet and ethanol induces a modest regeneration response

Chronic exposure to ethanol has been shown to impair the hepatic regeneration responses(Wands et al., 1979) with lower numbers of Ki67 positive hepatocytes reported in patients with alcohol related cirrhosis compared to other etiologies(Horiguchi et al., 2007). This leads to a compensatory ductular reaction in an attempt to restore the functioning hepatocyte pool(Dubuquoy et al., 2015) and indeed the extent of this response correlates with mortality in patients with alcoholic hepatitis(Gao and Shah, 2015; Sancho-Bru et al., 2012). To determine whether hepatocyte regeneration was triggered by our acute injury, we stained sections from matched anatomical lobes from our mouse livers with Ki67 antibody (see representative images in Figure 4) and showed that 15 days exposure to LdC diet plus ethanol was sufficient to stimulate hepatocyte proliferation whilst LdC diet alone had no

effect. Again although both WT and *Nrf2*$^{-/-}$ mice exhibited a similar magnitude of response upon quantitation, there was significant variation between fields of view within and between individual animals. Of note the extent and nature of Ki67 staining was similar at day 17 (see representative images in Supplemental Figure 4).

Administration of LdC diet plus ethanol alters hepatic metabolic profile

To characterise the mechanisms underlying the steatotic response observed in our animals we performed a detailed metabolomic characterisation using 1D-NMR on livers from WT mice fed either LdC diet alone or LdC diet plus ethanol. Livers were collected over the final five days of the protocol. We analysed samples from day 13 and 15, when the degree of injury was greatest, and at day 17 when ethanol was no longer present. The LdC diet alone sample was collected at Day 17 to allow comparison between chronic effects of diet exposure with and without ethanol. Figure 5 shows that we were able to characterize over 30 metabolites within the samples. These included amino acids, organic acids, phospholipids and nucleotides. For clarity these are divided into categories in Figure 5. Of note for many groups of metabolites there was a clear trend for increased content in livers during peak injury with a gradual return to baseline as ethanol was withdrawn. ANOVA confirmed there was a significant effect of ethanol on metabolite content. Intermediates in the metabolism of lipids, carbohydrates and amino acids were highest in ethanol-fed animals and declined to diet alone levels by day 17. Notable exceptions included maltose and formate that tended to increase over time and glucose, lactate and alanine that remained more or less static over time. Multiparametric statistical analysis confirmed that for most metabolites there is no significant difference between metabolite classes at day 17 on LdC alone vs Day 17 after withdrawal of alcohol. Interestingly however amino acid metabolism was different, and here at day 17 there is still a significant difference in expression between animals exposed to diet alone and those which had received ethanol (Figure 5).

Discussion

Rodent models of alcoholic hepatitis are of significant importance for new drug discovery in an area of unmet clinical need. However, many models don't recreate all the systemic sequlae, fall outside of local regulatory requirements or are technically challenging to operate. Hence each model has its own individual challenges and specific advantages (reviewed in(Wilkin et al., 2016)). We have based our protocol on one of the most widely

used models, the NIAAA binge model(Bertola et al., 2013a) which is similarly easy to perform and involves administration of ethanol in a high fat liquid diet with a final binge dose of ethanol before collection. This model had no mortality and a reasonable biochemical response but there is little hepatic inflammation and no fibrosis demonstrable in mice on this protocol(Bertola et al., 2013a).

This poor recreation of human disease presentation in the most widely used models has led to disappointing outcomes in clinical trials. For example there are cases where therapeutic anti-inflammatory targets identified as a consequence of rodent studies have not shown success when translated into a human setting(Woolbright and Jaeschke, 2018). Recent evidence suggested that *Nrf*2-/- mice are more sensitive to oxidant-mediated injury, and exhibit a reproducible alcohol-related injury even on relatively simple dietary administration protocols. *Nrf2* is a regulator of cellular responses to oxidative stress that is highly expressed in the liver where it plays a protective effect in the context of alcohol exposure(Sun et al., 2018). *Nrf2* -/- mice are more sensitive to the effects of ethanol and exhibit exaggerated hypothermic and hypoglycemic responses and reduced capability to metabolise acetaldehyde(Sun et al., 2018). They also have a higher mortality on binge ethanol models. It is notable therefore that we did not see dramatic differences between injury in our wild type vs *Nrf2*$^{-/-}$ animals. In the previous study(Lamle et al., 2008) the authors used male animals and commenced the protocol with young animals (6-8 weeks). The ethanol content of the liquid diet was gradually increased as we did up to a maximum of 6.3% and administered a single daily ethanol gavage. We observed a similar weight-loss and development of steatosis but Lamle *et al.,(Lamle et al., 2008)* noted that many animals became moribund after gavage and also had a significant mortality (all *Nrf2*$^{-/-}$ animals died by day 24). Typical serum ALT levels exceeded 3000IU/L in the *Nrf2*$^{-/-}$ animals in the Lamle study. We did see this in some animals but our mean *Nrf2*$^{-/-}$ injury peaked at around 1000IU/L for ALT. We surmise that the difference may relate to the welfare regulations which we operate under in the UK. We cannot run experiments to a mortality endpoint and thus tended to start our experimental protocol with older, heavier mice (typically 10-12 weeks and around 20g). This led to less weight loss as a percentage of starting mass and also meant that mice tolerated the gavages and alcohol exposure better. Thus, we would suggest our injury was more modest but sustainable. Similarly our use of female animals (in both WT and *Nrf2*$^{-/-}$ groups) likely accounts for the injury in our WT cohort (in contrast to the Lamle study(Lamle et al., 2008)).

Previous studies also suggest that human females have an increased susceptibility to alcohol-related liver injury(Eagon, 2010) and female mice tend to consume more alcohol than mice on same protocol(Gelineau et al., 2017). Female mice have higher activities of

alcohol metabolising enzymes and thus faster rates of ethanol metabolism and clearance compared to males(Kishimoto et al., 2002). Female mice have been shown to achieve higher plasma alcohol concentration and get more significant steatosis and triglyceride increases than males on the same protocol(Wagnerberger et al., 2013). Thus, we considered it interesting to see how female WT mice compared to *Nrf2*-deficient animals on our protocol. Our results showed that using a combination of LdC diet +/- EtOH combined with more frequent additional EtOH gavage than used in the NIAAA model could reproduce many of the key features of alcoholic hepatitis in a murine model. Mice treated with ethanol developed a significant elevation in serum transaminases, with significant steatosis and a hepatic neutrophil infiltrate. This model is relatively easier to set up than the intragastric infusion model described by Tsukamoto et al(Tsukamoto et al., 1985b), and is reasonably tolerated - very few mice reached the experimental or humane end-points prior to the planned completion date. Our framework for animal use in the UK means we cannot run experiments to a mortality endpoint, but we did observe that the small frequency of animals which reached the humane endpoints was similar between WT and *Nrf2-/-* animals. Interestingly we did not see significantly greater injury in our female *Nrf2-/-* mice compared to WT females according to the parameters we assessed. Nevertheless, WT females were more reproducible as a group within each analysis than the female *Nrf2* mice with virtually the same extent of injury. This may reflect the relatively mild injuries imposed by UK ethical standards for alcohol models but supports the concept that female mice are particularly susceptible to alcohol injury(Wagnerberger et al., 2013) and eliminates the need to use *Nrf2-/-* mice.

In our study, AST and ALT levels were greater than five times the baseline levels with AST>ALT. In humans relatively modest increases in serum transaminases are seen in AH with AST>ALT a characteristic diagnostic criteria(Botros and Sikaris, 2013). Humans also present with elevated bilirubin and hepatic neutrophil infiltration(Woolbright and Jaeschke, 2018) with fibrosis being a common feature. In agreement with many other models we did not see elevated serum bilirubin levels, but our transaminase levels and incipient fibrosis stand apart (Woolbright and Jaeschke, 2018). In mice neutrophils normally only constitute about 10-25% of peripheral immune cells so our peripheral increases in AH are significant and accompanied by a proportional decrease in circulating lymphocytes. This model induces increased hepatic recruitment of neutrophils, characteristic of ethanol-mediated liver injury, which is a prominent clinical feature of AH in humans and correlates with disease prognosis(Degre et al., 2012; Dominguez et al., 2009).Thus we are recreating the picture seen in acute human alcoholic hepatitis where the ethanol causes a transient increase in circulating myeloid cell populations(Gao et al., 2019) and a profound neutrophil and myeloid

cell inflammation in the damaged liver. Indeed the circulating neutrophil: lymphocyte ratio has prognostic relevance in alcoholic hepatitis(Forrest et al., 2019). However we did not see particularly dense neutrophil infiltrates, abundant ballooning, cholestasis or Mallory-Denk bodies(Altamirano et al., 2014), which would characterise severe acute human alcoholic hepatitis. This likely relates to the short duration of our injury. It is important to note that we have quantified lymphoid and myeloid cells as a proportion of total peripheral blood or hepatic immune cells and thus absolute numerical increases in hepatic cells under inflamed conditions may be underestimated. However this was sufficient to cause systemic responses (weight loss, neutrophilia) and hepatic metabolic changes(Brandl et al., 2018; Ding et al., 2019; Latchoumycandane et al., 2014) (elevated taurine, lactate and glycerol) that do recreate the human picture.

Previous studies of mice on high fat diet suggest that female animals are more resistant to the metabolic sequale of these diets with decreased weight gain, insulin secretion and better glucose tolerance than male mice(Gelineau et al., 2017). Thus, separation of effects of ethanol as opposed to high fat diet may be easier in female animals. Our model using female mice incorporates administration of a Lieber deCarli ethanol diet that contains maltose dextrin and escalating concentrations of ethanol. This model causes a predictable steatosis driven by increased hepatic free fatty acid uptake, *de novo* lipogenesis and impaired beta oxidation(Warner et al., 2018) and lipolysis, which is rapidly reversed on withdrawal of ethanol(Thomes et al., 2019). There appeared to be a tendency for metabolites to peak at day 13 and decline therafter, rather than continuing to increase to the final day of ethanol exposure at day 15. This may reflect different timepoints of sample collection within our small cohorts of animals, as there is a clear diurnal regulation of murine metabolism and feeding habits(Weger et al., 2019), which are impacted upon by ethanol exposure(Gaucher et al., 2019). The effect may also be related to time of collection after administration of final ethanol gavage. Increased energy availability in mice fed diet plus ethanol led to accumulation of fuel for DNL and the tricarboxylic acid (TCA) cycle explaining our observed accumulation of lipid in hepatocytes. We also noted that the response was rapidly reversable upon withdrawal of ethanol. Impaired carbohydrate metabolism and ketoacidosis are a common feature in patients admitted with alcoholic hepatitis(Wrenn et al., 1991) and features of our murine hepatic metabolic profile suggest we are recreating this response. It is suggested that hepatocytes preferentially use glycerol as a substrate for gluconeogenesis(Kalemba et al., 2019) and thus our increase in glycerol may suggest impaired glucose generation. This combined with static lactate concentration hints at reduced pyruvate generation ability and inhibition of gluconeogenesis. Finally, our increased hepatic 3 hyroxybutyrate concentration is suggestive of alcohol-induced

ketoacidosis(Srinivasan et al., 2019) and suppression of gluconeogenesis. We observed increased accumulation of taurine during ethanol exposure and hepatic and peripheral increases in taurine content during ethanol injury have been reported by other groups(Kerai et al., 1998). Additionally, taurine can suppress inflammation and reduce oxidative stress(Balkan et al., 2002) therefore our hepatic increase may indicate activation of hepatoprotective mechanisms. Consequently, our metabolic profiling supports the steatosis we observe in mice on diet and fits with the phenotype of patients exposed to alcohol. The only notable exception is the increasing hepatic abundance of maltose, which was derived from the maltose dextran used in maintenance of isocaloric intake.

The degree of fibrosis in this model was mild, whereas patients with alcoholic hepatitis often exhibit centrilobular pericellular/sclerosing fibrosis which may extend to cirrhosis as a consequence of ongoing acute on chronic alcohol-related injury. Unfortunately, advanced fibrosis is not reported in any of the murine models of AH. Extending the duration or concentration of ethanol administration would potentially induce a more severe fibrosis. However, this would be practically difficult within the UK legislative framework because of weight loss approaching 20% around day 15. Other possible methods that could be considered to increase the severity of fibrosis include use of carbon tetrachloride injections to induce fibrosis, or possibly a longer duration of the LdC diet administration prior to giving ethanol. Given our evidence that some degree of hepatocyte regeneration occurs within our timeframe (Figure 4) it would also be possible to exacerbate the injury by compromising normal regenerative mechanisms during ongoing injury(Raven et al., 2017).

We originally hypothesized that mice deficient in *Nrf2* may show an altered fibrogenic response. Whilst Xie *et al*., report that the *Nrf2*-Keap-ARE1 pathway protects against fibrogenesis(Xie et al., 2018), Hernandez -gea *et al*., have shown that inhibition of *Nrf2* function in stellate cells reduces their fibrogenic potential(Hernandez-Gea et al., 2013). In our hands, the degree of fibrosis assessed by PSR staining was not significantly different between WT and *Nrf2*$^{-/-}$ mice on LdC plus EtOH protocol, which suggests that, at least in this model the role is minimal. However, we did note that the significant increase we observed in PSR staining between LdC alone and LdC+ethanol in WT mice was not recreated in the *Nrf2*$^{-/-}$ mice (i.e there was similar extent of staining in both conditions) this may suggest that the *Nrf2* deficiency has indeed modified stellate cell activation. Persistent activation of *Nrf2-/-* in a situation of impaired hepatic autophagy is important for inflammation, fibrogenesis and apoptosis and is linked to tumorigenesis (Ni et al., 2014). Although deficiency in *Nrf2* may increase reactive oxygen species (ROS) induced hepatic damage, and thus has been linked to more severe alcohol-dependent injury in some models(Lamle et al., 2008), it may be unwise to use these mice when modelling injuries linked to fibrogenesis or longer term liver

injury. Anecdotally we also noted that the *Nrf2*$^{-/-}$ mice tended to be more aggressive, or at least to show diminished healing responses to injuries sustained in territorial fights. This is in keeping with reports of impaired wound healing responses in this strain(Li et al., 2019; Long et al., 2016) and influenced our opinions on the relative merits of this strain for modelling alcohol injury.However, we would note that the responses we have observed were generated from relatively small cohorts of animals housed in our specific facility and thus it is possible that using increased numbers of animals or those housed in alternate colonies may explain differential sensitivities of the *Nrf2* strain in different models.

There are a number of challenges of modelling human alcoholic hepatitis using mice. The alcohol catabolism rate is up to five-times higher in rodents compared to humans and the amount of ethanol administered to animals to achieve sustained blood alcohol concentration and subsequent liver injury cannot be directly compared with human alcohol consumption(Holmes et al., 1986). In a time course experiment, we found that upon withdrawal of ethanol at day 15 of this protocol, mice had normalisation of serum transaminases and were gaining weight again by day 17. Similarly, our reported metabolic changes began to normalise by day 17. Such rapid resolution of liver injury would not be typical of patients with severe alcoholic hepatitis. However, our use of female wild type mice has recreated many of the key features of human alcoholic hepatitis and thus has potential for improving our understanding of the proinflammatory, profibrotic and metabolic disturbances that characterise human disease.

References

Altamirano, J., Miquel, R., Katoonizadeh, A., Abraldes, J. G., Duarte-Rojo, A., Louvet, A., Augustin, S., Mookerjee, R. P., Michelena, J., Smyrk, T. C. et al. (2014). A histologic scoring system for prognosis of patients with alcoholic hepatitis. *Gastroenterology* **146**, 1231-9 e1-6.

AoM., S. (2004). Calling time – The nation's drinking as a major health issue. London.

Balkan, J., Kanbagli, O., Aykac-Toker, G. and Uysal, M. (2002). Taurine treatment reduces hepatic lipids and oxidative stress in chronically ethanol-treated rats. *Biol Pharm Bull* **25**, 1231-3.

Bertola, A., Mathews, S., Ki, S. H., Wang, H. and Gao, B. (2013a). Mouse model of chronic and binge ethanol feeding (the NIAAA model). *Nature protocols* **8**, 627-37.

Bertola, A., Park, O. and Gao, B. (2013b). Chronic plus binge ethanol feeding synergistically induces neutrophil infiltration and liver injury in mice: a critical role for E-selectin. *Hepatology* **58**, 1814-23.

Botros, M. and Sikaris, K. A. (2013). The de ritis ratio: the test of time. *Clin Biochem Rev* **34**, 117-30.

Brandl, K., Hartmann, P., Jih, L. J., Pizzo, D. P., Argemi, J., Ventura-Cots, M., Coulter, S., Liddle, C., Ling, L., Rossi, S. J. et al. (2018). Dysregulation of serum bile acids and FGF19 in alcoholic hepatitis. *Journal of hepatology* **69**, 396-405.

Chang, B., Xu, M. J., Zhou, Z., Cai, Y., Li, M., Wang, W., Feng, D., Bertola, A., Wang, H., Kunos, G. et al. (2015). Short- or long-term high-fat diet feeding plus acute ethanol binge synergistically induce acute liver injury in mice: an important role for CXCL1. *Hepatology* **62**, 1070-85.

Degre, D., Lemmers, A., Gustot, T., Ouziel, R., Trepo, E., Demetter, P., Verset, L., Quertinmont, E., Vercruysse, V., Le Moine, O. et al. (2012). Hepatic expression of CCL2 in alcoholic liver disease is associated with disease severity and neutrophil infiltrates. *Clin Exp Immunol* **169**, 302-10.

Denk, H., Franke, W. W., Kerjaschki, D. and Eckerstorfer, R. (1979). Mallory bodies in experimental animals and man. *Int Rev Exp Pathol* **20**, 77-121.

Denk, H., Stumptner, C. and Zatloukal, K. (2000). Mallory bodies revisited. *Journal of hepatology* **32**, 689-702.

Ding, Y., Yanagi, K., Cheng, C., Alaniz, R. C., Lee, K. and Jayaraman, A. (2019). Interactions between gut microbiota and non-alcoholic liver disease: The role of microbiota-derived metabolites. *Pharmacol Res* **141**, 521-529.

Dominguez, M., Miquel, R., Colmenero, J., Moreno, M., Garcia-Pagan, J. C., Bosch, J., Arroyo, V., Gines, P., Caballeria, J. and Bataller, R. (2009). Hepatic expression of CXC chemokines predicts portal hypertension and survival in patients with alcoholic hepatitis. *Gastroenterology* **136**, 1639-50.

Dubuquoy, L., Louvet, A., Lassailly, G., Truant, S., Boleslawski, E., Artru, F., Maggiotto, F., Gantier, E., Buob, D., Leteurtre, E. et al. (2015). Progenitor cell expansion and impaired hepatocyte regeneration in explanted livers from alcoholic hepatitis. *Gut* **64**, 1949-60.

Eagon, P. K. (2010). Alcoholic liver injury: influence of gender and hormones. *World journal of gastroenterology : WJG* **16**, 1377-84.

European Association for the Study of, L. (2012). EASL clinical practical guidelines: management of alcoholic liver disease. *Journal of hepatology* **57**, 399-420.

Forrest, E. H., Storey, N., Sinha, R., Atkinson, S. R., Vergis, N., Richardson, P., Masson, S., Ryder, S., Thursz, M. R., Allison, M. et al. (2019). Baseline neutrophil-to-lymphocyte ratio predicts response to corticosteroids and is associated with infection and renal dysfunction in alcoholic hepatitis. *Alimentary pharmacology & therapeutics* **50**, 442-453.

Gao, B., Ahmad, M. F., Nagy, L. E. and Tsukamoto, H. (2019). Inflammatory pathways in alcoholic steatohepatitis. *Journal of hepatology* **70**, 249-259.

Gao, B. and Shah, V. H. (2015). Combination therapy: New hope for alcoholic hepatitis? *Clinics and research in hepatology and gastroenterology* **39 Suppl 1**, S7-S11.

Gaucher, J., Kinouchi, K., Ceglia, N., Montellier, E., Peleg, S., Greco, C. M., Schmidt, A., Forne, I., Masri, S., Baldi, P. et al. (2019). Distinct metabolic adaptation of liver circadian pathways to acute and chronic patterns of alcohol intake. *Proceedings of the National Academy of Sciences of the United States of America* **116**, 25250-25259.

Gelineau, R. R., Arruda, N. L., Hicks, J. A., Monteiro De Pina, I., Hatzidis, A. and Seggio, J. A. (2017). The behavioral and physiological effects of high-fat diet and alcohol consumption: Sex differences in C57BL6/J mice. *Brain Behav* **7**, e00708.

Han, H., Hu, J., Lau, M. Y., Feng, M., Petrovic, L. M. and Ji, C. (2013). Altered methylation and expression of ER-associated degradation factors in long-term alcohol and constitutive ER stress-induced murine hepatic tumors. *Front Genet* **4**, 224.

Hernandez-Gea, V., Hilscher, M., Rozenfeld, R., Lim, M. P., Nieto, N., Werner, S., Devi, L. A. and Friedman, S. L. (2013). Endoplasmic reticulum stress induces fibrogenic activity in hepatic stellate cells through autophagy. *J Hepatol* **59**, 98-104.

Hmoud, B. S., Patel, K., Bataller, R. and Singal, A. K. (2016). Corticosteroids and occurrence of and mortality from infections in severe alcoholic hepatitis: a meta-analysis of randomized trials. *Liver international : official journal of the International Association for the Study of the Liver* **36**, 721-8.

Holmes, R. S., Duley, J. A., Algar, E. M., Mather, P. B. and Rout, U. K. (1986). Biochemical and genetic studies on enzymes of alcohol metabolism: the mouse as a model organism for human studies. *Alcohol and alcoholism* **21**, 41-56.

Horiguchi, N., Ishac, E. J. and Gao, B. (2007). Liver regeneration is suppressed in alcoholic cirrhosis: correlation with decreased STAT3 activation. *Alcohol* **41**, 271-80.

Hu, M., Yin, H., Mitra, M. S., Liang, X., Ajmo, J. M., Nadra, K., Chrast, R., Finck, B. N. and You, M. (2013). Hepatic-specific lipin-1 deficiency exacerbates experimental alcohol-induced steatohepatitis in mice. *Hepatology* **58**, 1953-63.

Ji, C., Chan, C. and Kaplowitz, N. (2006). Predominant role of sterol response element binding proteins (SREBP) lipogenic pathways in hepatic steatosis in the murine intragastric ethanol feeding model. *Journal of hepatology* **45**, 717-24.

Ji, C., Deng, Q. and Kaplowitz, N. (2004). Role of TNF-alpha in ethanol-induced hyperhomocysteinemia and murine alcoholic liver injury. *Hepatology* **40**, 442-51.

Kalemba, K. M., Wang, Y., Xu, H., Chiles, E., McMillin, S. M., Kwon, H., Su, X. and Wondisford, F. E. (2019). Glycerol induces G6pc in primary mouse hepatocytes and is the preferred substrate for gluconeogenesis both in vitro and in vivo. *The Journal of biological chemistry* **294**, 18017-18028.

Kerai, M. D., Waterfield, C. J., Kenyon, S. H., Asker, D. S. and Timbrell, J. A. (1998). Taurine: protective properties against ethanol-induced hepatic steatosis and lipid peroxidation during chronic ethanol consumption in rats. *Amino Acids* **15**, 53-76.

Ki, S. H., Park, O., Zheng, M., Morales-Ibanez, O., Kolls, J. K., Bataller, R. and Gao, B. (2010). Interleukin-22 treatment ameliorates alcoholic liver injury in a murine model of chronic-binge ethanol feeding: role of signal transducer and activator of transcription 3. *Hepatology* **52**, 1291-300.

Kirpich, I. A., Feng, W., Wang, Y., Liu, Y., Barker, D. F., Barve, S. S. and McClain, C. J. (2012). The type of dietary fat modulates intestinal tight junction integrity, gut permeability, and hepatic toll-like receptor expression in a mouse model of alcoholic liver disease. *Alcoholism, clinical and experimental research* **36**, 835-46.

Kishimoto, R., Ogishi, Y., Ueda, M., Matsusaki, M., Amako, K., Goda, K. and Park, S. S. (2002). Gender-related differences in mouse hepatic ethanol metabolism. *J Nutr Sci Vitaminol (Tokyo)* **48**, 216-24.

Kleiner, D. E., Brunt, E. M., Van Natta, M., Behling, C., Contos, M. J., Cummings, O. W., Ferrell, L. D., Liu, Y. C., Torbenson, M. S., Unalp-Arida, A. et al. (2005). Design and validation of a histological scoring system for nonalcoholic fatty liver disease. *Hepatology.* **41**, 1313-1321.

Kong, X., Yang, Y., Ren, L., Shao, T., Li, F., Zhao, C., Liu, L., Zhang, H., McClain, C. J. and Feng, W. (2017). Activation of autophagy attenuates EtOH-LPS-induced hepatic steatosis and injury through MD2 associated TLR4 signaling. *Sci Rep* **7**, 9292.

Lamle, J., Marhenke, S., Borlak, J., von Wasielewski, R., Eriksson, C. J., Geffers, R., Manns, M. P., Yamamoto, M. and Vogel, A. (2008). Nuclear factor-eythroid 2-related factor 2 prevents alcohol-induced fulminant liver injury. *Gastroenterology* **134**, 1159-68.

Latchoumycandane, C., Nagy, L. E. and McIntyre, T. M. (2014). Chronic ethanol ingestion induces oxidative kidney injury through taurine-inhibitable inflammation. *Free radical biology & medicine* **69**, 403-16.

Lazaro, R., Wu, R., Lee, S., Zhu, N. L., Chen, C. L., French, S. W., Xu, J., Machida, K. and Tsukamoto, H. (2015). Osteopontin deficiency does not prevent but promotes alcoholic neutrophilic hepatitis in mice. *Hepatology* **61**, 129-40.

Li, H. H., Tyburski, J. B., Wang, Y. W., Strawn, S., Moon, B. H., Kallakury, B. V., Gonzalez, F. J. and Fornace, A. J., Jr. (2014). Modulation of fatty acid and bile acid metabolism by peroxisome proliferator-activated receptor alpha protects against alcoholic liver disease. *Alcoholism, clinical and experimental research* **38**, 1520-31.

Li, M., Yu, H., Pan, H., Zhou, X., Ruan, Q., Kong, D., Chu, Z., Li, H., Huang, J., Huang, X. et al. (2019). Nrf2 Suppression Delays Diabetic Wound Healing Through Sustained Oxidative Stress and Inflammation. *Front Pharmacol* **10**, 1099.

Long, M., Rojo de la Vega, M., Wen, Q., Bharara, M., Jiang, T., Zhang, R., Zhou, S., Wong, P. K., Wondrak, G. T., Zheng, H. et al. (2016). An Essential Role of NRF2 in Diabetic Wound Healing. *Diabetes* **65**, 780-93.

Louvet, A., Thursz, M. R., Kim, D. J., Labreuche, J., Atkinson, S. R., Sidhu, S. S., O'Grady, J. G., Akriviadis, E., Sinakos, E., Carithers, R. L., Jr. et al. (2018). Corticosteroids Reduce Risk of Death Within 28 Days for Patients With Severe Alcoholic Hepatitis, Compared With Pentoxifylline or Placebo-a Meta-analysis of Individual Data From Controlled Trials. *Gastroenterology* **155**, 458-468 e8.

Mathurin, P. (2005). Corticosteroids for alcoholic hepatitis--what's next? *J Hepatol* **43**, 526-33.

Ni, H. M., Woolbright, B. L., Williams, J., Copple, B., Cui, W., Luyendyk, J. P., Jaeschke, H. and Ding, W. X. (2014). Nrf2 promotes the development of fibrosis and tumorigenesis in mice with defective hepatic autophagy. *Journal of hepatology* **61**, 617-25.

Preedy, V. R., Duane, P. and Peters, T. J. (1988). Biological effects of chronic ethanol consumption: a reappraisal of the Lieber-De Carli liquid-diet model with reference to skeletal muscle. *Alcohol and alcoholism* **23**, 151-4.

Raven, A., Lu, W. Y., Man, T. Y., Ferreira-Gonzalez, S., O'Duibhir, E., Dwyer, B. J., Thomson, J. P., Meehan, R. R., Bogorad, R., Koteliansky, V. et al. (2017). Cholangiocytes act as facultative liver stem cells during impaired hepatocyte regeneration. *Nature* **547**, 350-354.

Ronis, M. J., Mercer, K. E., Gannon, B., Engi, B., Zimniak, P., Shearn, C. T., Orlicky, D. J., Albano, E., Badger, T. M. and Petersen, D. R. (2015). Increased 4-hydroxynonenal protein adducts in male GSTA4-4/PPAR-alpha double knockout mice enhance injury during early stages of alcoholic liver disease. *American journal of physiology. Gastrointestinal and liver physiology* **308**, G403-15.

Saborano, R., Eraslan, Z., Roberts, J., Khanim, F. L., Lalor, P. F., Reed, M. A. C. and Gunther, U. L. (2019). A framework for tracer-based metabolism in mammalian cells by NMR. *Sci Rep* **9**, 2520.

Sancho-Bru, P., Altamirano, J., Rodrigo-Torres, D., Coll, M., Millan, C., Jose Lozano, J., Miquel, R., Arroyo, V., Caballeria, J., Gines, P. et al. (2012). Liver progenitor cell markers correlate with liver damage and predict short-term mortality in patients with alcoholic hepatitis. *Hepatology* **55**, 1931-41.

Schofield, Z., Reed, M. A., Newsome, P. N., Adams, D. H., Gunther, U. L. and Lalor, P. F. (2017). Changes in human hepatic metabolism in steatosis and cirrhosis. *World journal of gastroenterology : WJG* **23**, 2685-2695.

Srinivasan, M. P., Shawky, N. M., Kaphalia, B. S., Thangaraju, M. and Segar, L. (2019). Alcohol-induced ketonemia is associated with lowering of blood glucose, downregulation of gluconeogenic genes, and depletion of hepatic glycogen in type 2 diabetic db/db mice. *Biochemical pharmacology* **160**, 46-61.

Sun, J., Fu, J., Li, L., Chen, C., Wang, H., Hou, Y., Xu, Y. and Pi, J. (2018). Nrf2 in alcoholic liver disease. *Toxicology and applied pharmacology* **357**, 62-69.

Thomes, P. G., Rasineni, K., Yang, L., Donohue, T. M., Jr., Kubik, J. L., McNiven, M. A. and Casey, C. A. (2019). Ethanol withdrawal mitigates fatty liver by normalizing lipid catabolism. *American journal of physiology. Gastrointestinal and liver physiology* **316**, G509-G518.

Thursz, M. R., Forrest, E. H., Ryder, S. and investigators, S. (2015). Prednisolone or Pentoxifylline for Alcoholic Hepatitis. *The New England journal of medicine* **373**, 282-3.

Tsukamoto, H., French, S. W., Benson, N., Delgado, G., Rao, G. A., Larkin, E. C. and Largman, C. (1985a). Severe and progressive steatosis and focal necrosis in rat liver induced by continuous intragastric infusion of ethanol and low fat diet. *Hepatology* **5**, 224-32.

Tsukamoto, H., French, S. W., Reidelberger, R. D. and Largman, C. (1985b). Cyclical pattern of blood alcohol levels during continuous intragastric ethanol infusion in rats. *Alcoholism, clinical and experimental research* **9**, 31-7.

Wagnerberger, S., Fiederlein, L., Kanuri, G., Stahl, C., Millonig, G., Mueller, S., Bischoff, S. C. and Bergheim, I. (2013). Sex-specific differences in the development of acute alcohol-induced liver steatosis in mice. *Alcohol and alcoholism* **48**, 648-56.

Wands, J. R., Carter, E. A., Bucher, N. L. and Isselbacher, K. J. (1979). Inhibition of hepatic regeneration in rats by acute and chronic ethanol intoxication. *Gastroenterology* **77**, 528-31.

Warner, D. R., Liu, H., Ghosh Dastidar, S., Warner, J. B., Prodhan, M. A. I., Yin, X., Zhang, X., Feldstein, A. E., Gao, B., Prough, R. A. et al. (2018). Ethanol and unsaturated dietary fat induce unique patterns of hepatic omega-6 and omega-3 PUFA oxylipins in a mouse model of alcoholic liver disease. *PloS one* **13**, e0204119.

Weger, B. D., Gobet, C., Yeung, J., Martin, E., Jimenez, S., Betrisey, B., Foata, F., Berger, B., Balvay, A., Foussier, A. et al. (2019). The Mouse Microbiome Is Required for Sex-Specific Diurnal Rhythms of Gene Expression and Metabolism. *Cell metabolism* **29**, 362-382 e8.

Weston, C. J., Shepherd, E. L., Claridge, L. C., Rantakari, P., Curbishley, S. M., Tomlinson, J. W., Hubscher, S. G., Reynolds, G. M., Aalto, K., Anstee, Q. M. et al. (2015). Vascular adhesion protein-1 promotes liver inflammation and drives hepatic fibrosis. *The Journal of clinical investigation* **125**, 501-20.

Wieser, V., Adolph, T. E., Enrich, B., Kuliopulos, A., Kaser, A., Tilg, H. and Kaneider, N. C. (2017). Reversal of murine alcoholic steatohepatitis by pepducin-based functional blockade of interleukin-8 receptors. *Gut* **66**, 930-938.

Wilkin, R. J., Lalor, P. F., Parker, R. and Newsome, P. N. (2016). Murine Models of Acute Alcoholic Hepatitis and Their Relevance to Human Disease. *The American journal of pathology* **186**, 748-60.

Woolbright, B. L. and Jaeschke, H. (2018). Alcoholic Hepatitis: Lost in Translation. *J Clin Transl Hepatol* **6**, 89-96.

Wrenn, K. D., Slovis, C. M., Minion, G. E. and Rutkowski, R. (1991). The syndrome of alcoholic ketoacidosis. *The American journal of medicine* **91**, 119-28.

Xie, Z. Y., Xiao, Z. H. and Wang, F. F. (2018). Inhibition of autophagy reverses alcohol-induced hepatic stellate cells activation through activation of Nrf2-Keap1-ARE signaling pathway. *Biochimie* **147**, 55-62.

Zhang, H. and Meadows, G. G. (2008). Chronic alcohol consumption perturbs the balance between thymus-derived and bone marrow-derived natural killer cells in the spleen. *Journal of leukocyte biology* **83**, 41-7.

Figures

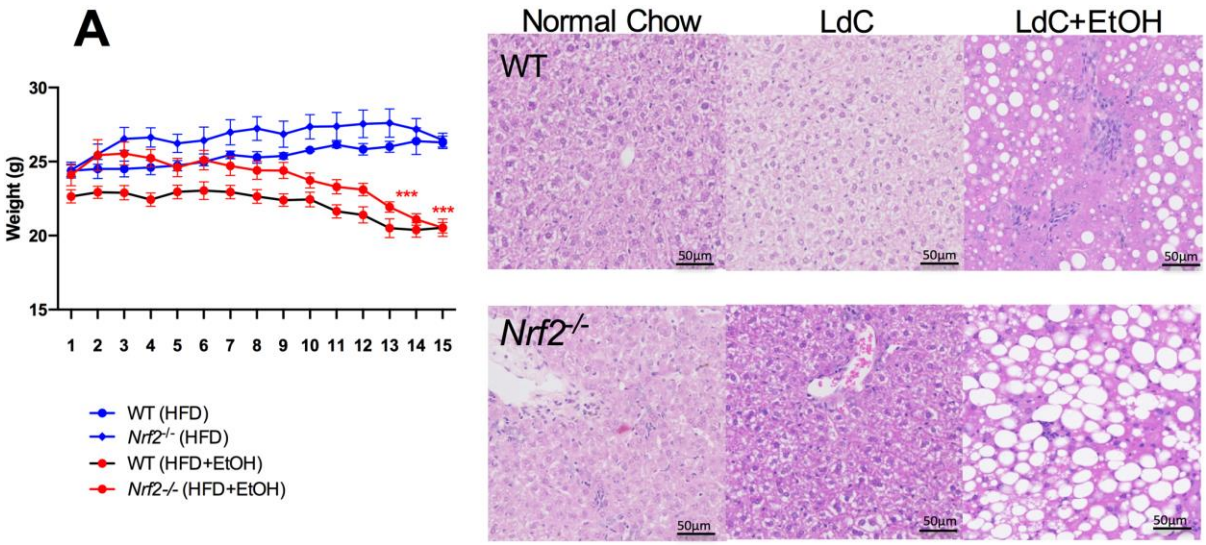

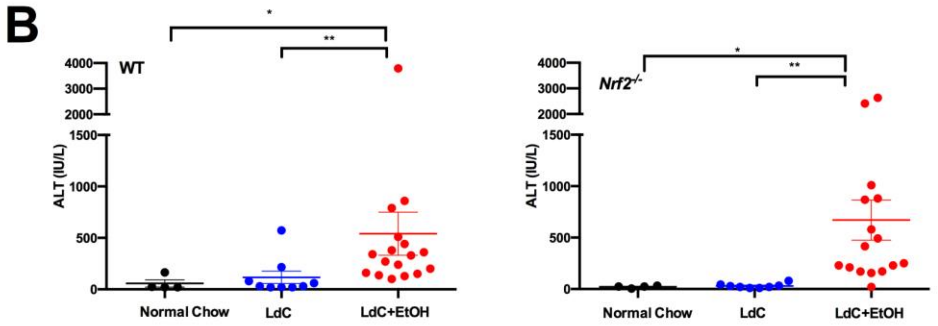

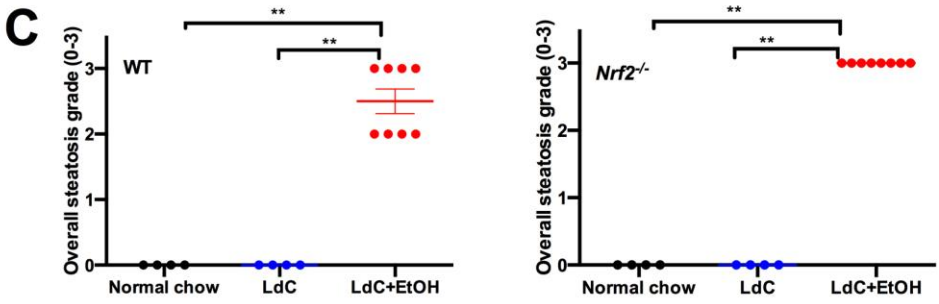

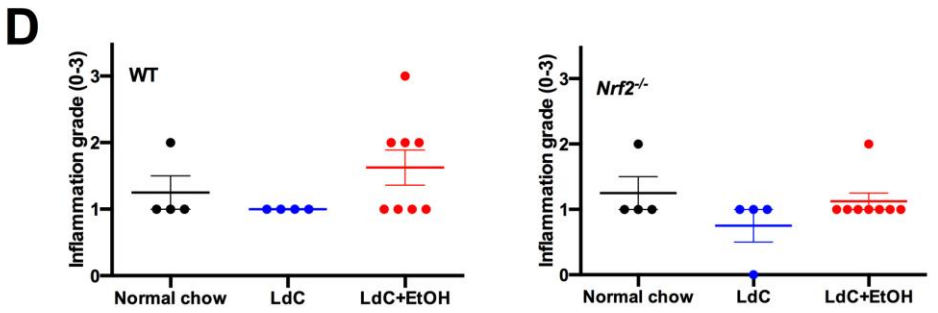

Figure 1: Mice treated with modified LdC diet and ethanol exhibit weight loss, inflammation and hepatic steatosis.

WT and *Nrf2*$^{-/-}$ mice were fed LdC diet only for 5 days. At day 6 experimental groups received 2.2% EtOH mixed into the LdC diet. This was increased to 4.4% at day 9, and to 6.3% at day 12. Additionally, experimental groups received twice daily ethanol gavage of 33% EtOH (LdC+EtOH). Control mice received LdC diet only throughout the experiment and were not gavaged. (A) left graph indicates mean mouse weight ±SEM in gram (g). Linear regression analysis confirmed significant weightloss in WT and *Nrf2*-/- mice on LdC+EtOH ($p < 0.01$ for both). Representative H&E stained liver sections from WT and *Nrf2*$^{-/-}$ mice fed normal chow, LdC or LdC+EtOH are shown (Right images). Scale bar is at 50µm, data is representative of at least n=6 animals per group. (B) Serum was prepared from WT and *Nrf2*$^{-/-}$ mice at day 15 for determination of ALT concentration. Symbols are values from individual mice and bars are mean ±SEM for the group. Statistical difference level is indicated by * for $p<0.05$ and ** for $p<0.01$ performed with the Kruskal-Wallis Dunn's multiple comparison test. (C) Haematoxylin and eosin stained sections were scored semi-quantitatively for the grade steatosis on a scale of 0-3. Symbols are values from individual mice and bars indicate mean ±SEM for each group. Statistical difference level is indicated by * for $p<0.05$ and ** for $p<0.01$ performed with the Kruskal-Wallis Dunn's multiple comparison test. (D) Haematoxylin and eosin stained sections were scored for inflammation using overall grade (1-3). Symbols are values from individual mice and bars represent mean ± SEM of the group.

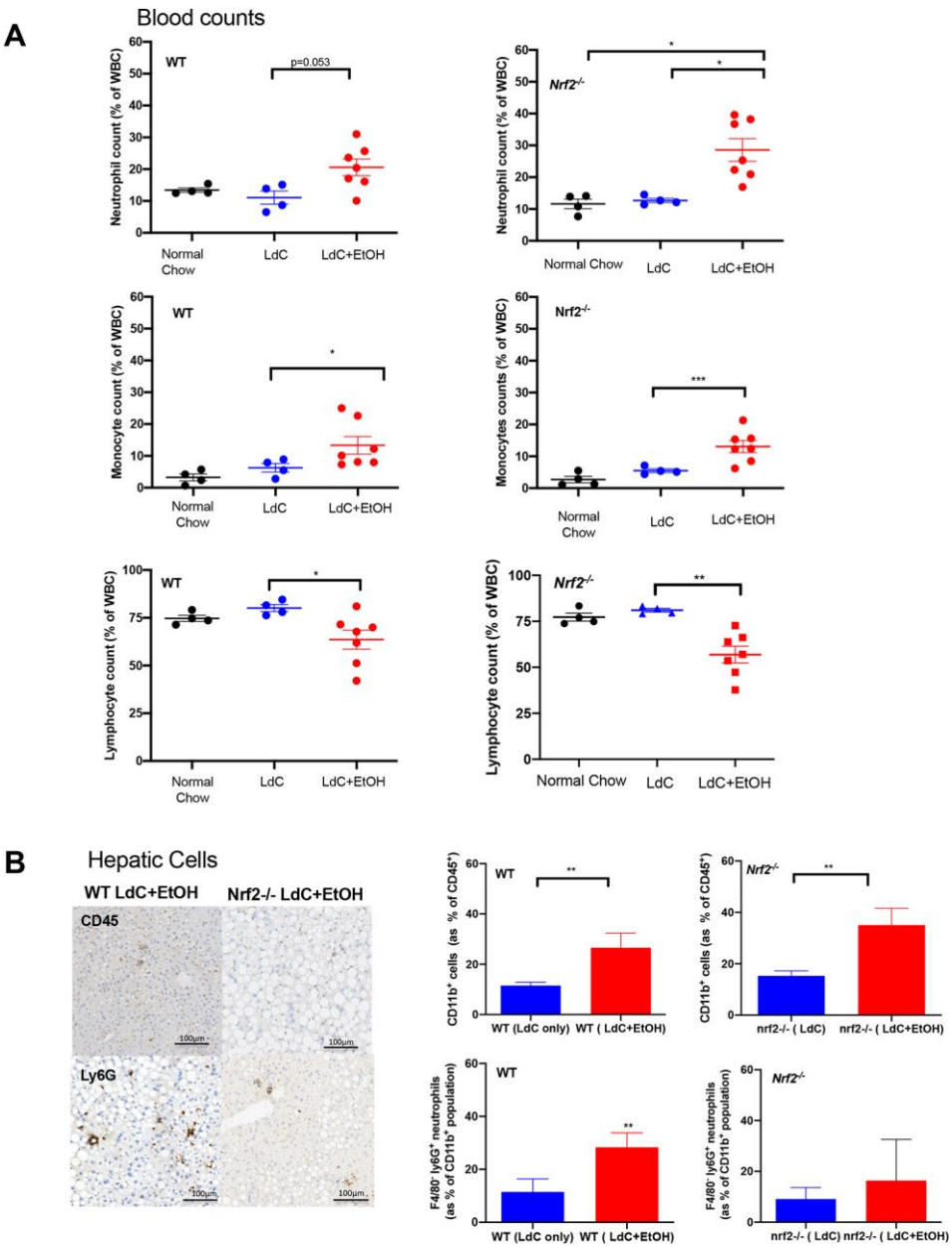

Figure 2: Injured WT and *Nrf2*$^{-/-}$ mice demonstrate alterations in peripheral and hepatic immune cell populations. A) Following cardiac puncture EDTA anti-coagulated blood was passed through an automated blood count analyser and neutrophil, monocyte and lymphocyte counts are presented as a percentage of WBC (white blood cells). Symbols are values from individual mice and bars represent mean ± SEM of the group . Statistical difference level is indicated by * for $p<0.05$ and ** for $p<0.01$ performed with the Kruskal-Wallis Dunn's multiple comparison test. B) Left Images : FFPE liver tissue was sectioned (5µm) and stained with anti-CD45, or Ly6G antibodies. In addition, liver lobes from mice fed with LdC or LdC+EtOH were collected at day 15 and digested for cytometric analysis (right graphs). Images are representative of multiple fields of view in n = 4-7 animals per group. Graphs show cytometric quantitation of myeloid cells (defined by live gating and then $CD45^{+}CD3^{-}CD11b^{+}$as a percentage of total CD45+ cells) and hepatic neutrophils (defined by live gating and then $CD45^{+}CD3^{-}F4/80^{-}Ly6G^{+}$ as a percentage of total CD11b+ cells) for WT and *Nrf2-/-* mice. Bars represent mean ± SEM of the group (n=4-7 individual livers per group. Statistical differences were assessed using Mann-Whitney test *$p < 0.05$, **$p < 0.01$.

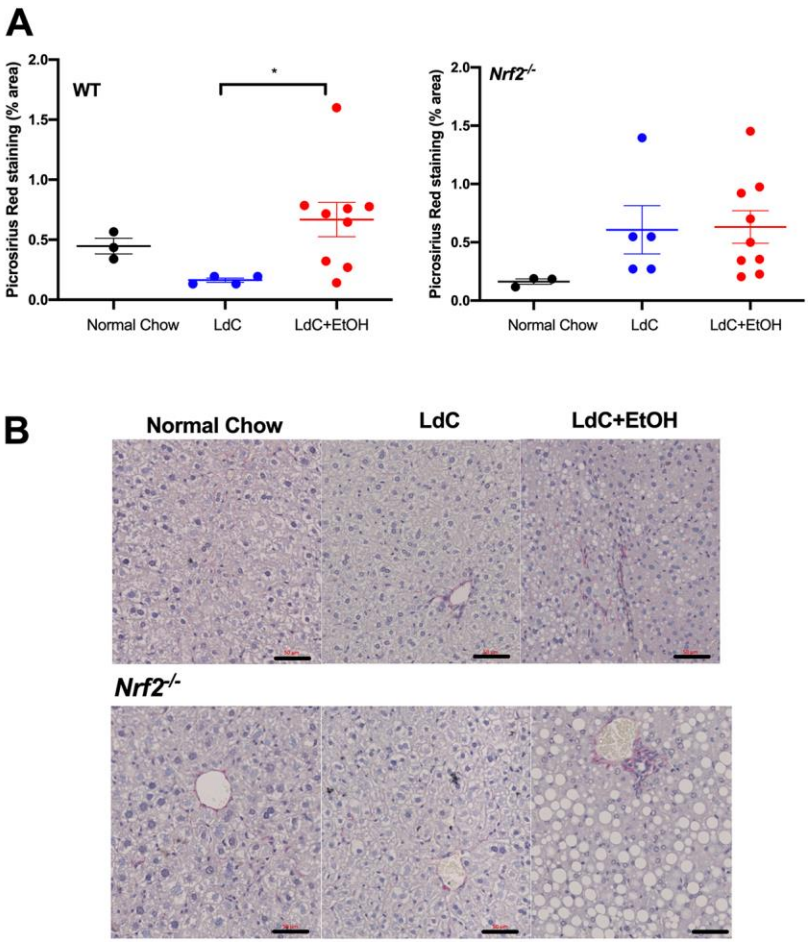

Figure 3: Mice receiving LdC diet and ethanol show signs of early fibrosis at day 15. FFPE liver tissue was sectioned (5µm) and stained with picrosirius red. For quantification 5-6 random fields of view per section were imaged and processed with ImageJ software. Data are expressed as the percentage of the total area of the section occupied by Sirius red staining. A) Average picrosirius red stained area in indicated groups of mice. Symbols are values from individual mice and bars represent mean ±SEM of the group. Statistical difference level is indicated by * for $p<0.05$ performed with Kruskal-Wallis Dunn's multiple comparison test. B) Representative images of picrosirius red-stained liver sections from WT and *Nrf2*$^{-/-}$ mice fed normal chow, LdC or LdC+EtOH are shown. Scale bar is at 50µm, data is representative of at least n=3 animals per group.

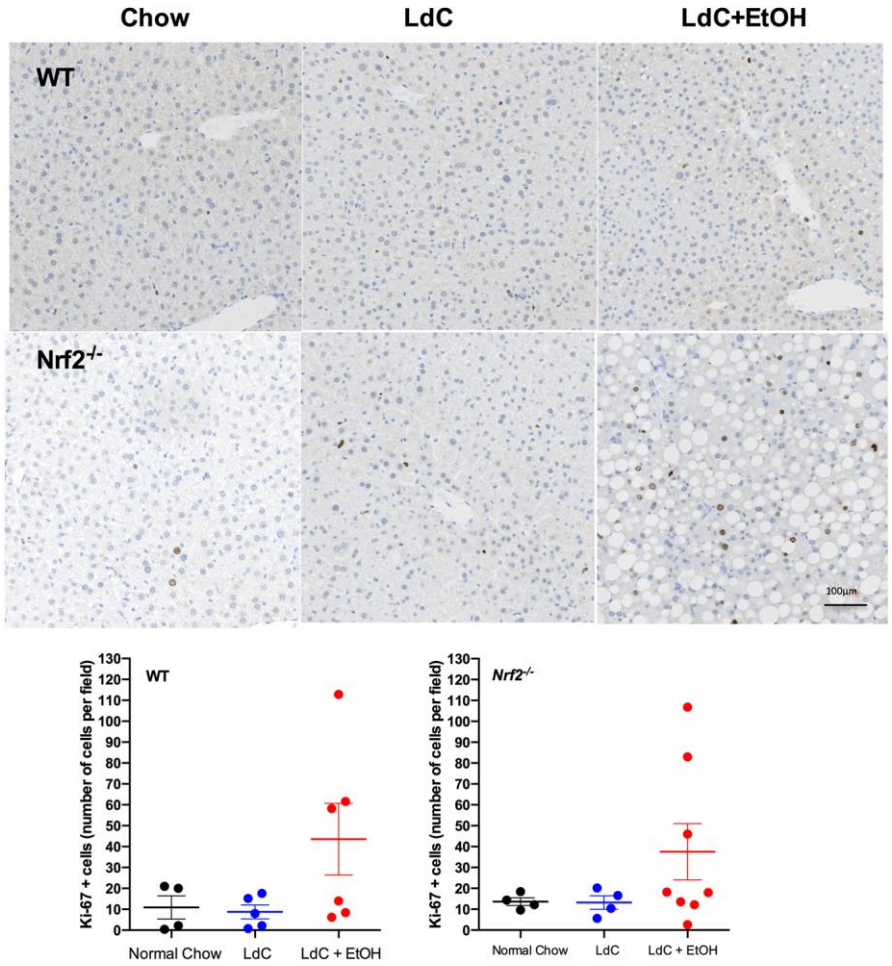

Figure 4: Ethanol induces an increase in hepatocyte proliferation. FFPE liver tissue was sectioned (5µm) and stained with Ki67 antibody to identify proliferating cells. Representative images of Ki67 stained liver sections from WT and *Nrf2*$^{-/-}$ mice fed normal chow, LdC or LdC+EtOH are shown. Scale bar is at 100µm, data is representative of at least n=4 animals per group. For quantification 5-6 random fields of view per section were imaged and processed with ImageJ software. Data was expressed as number of Ki67 positive hepatocytes per field of view.

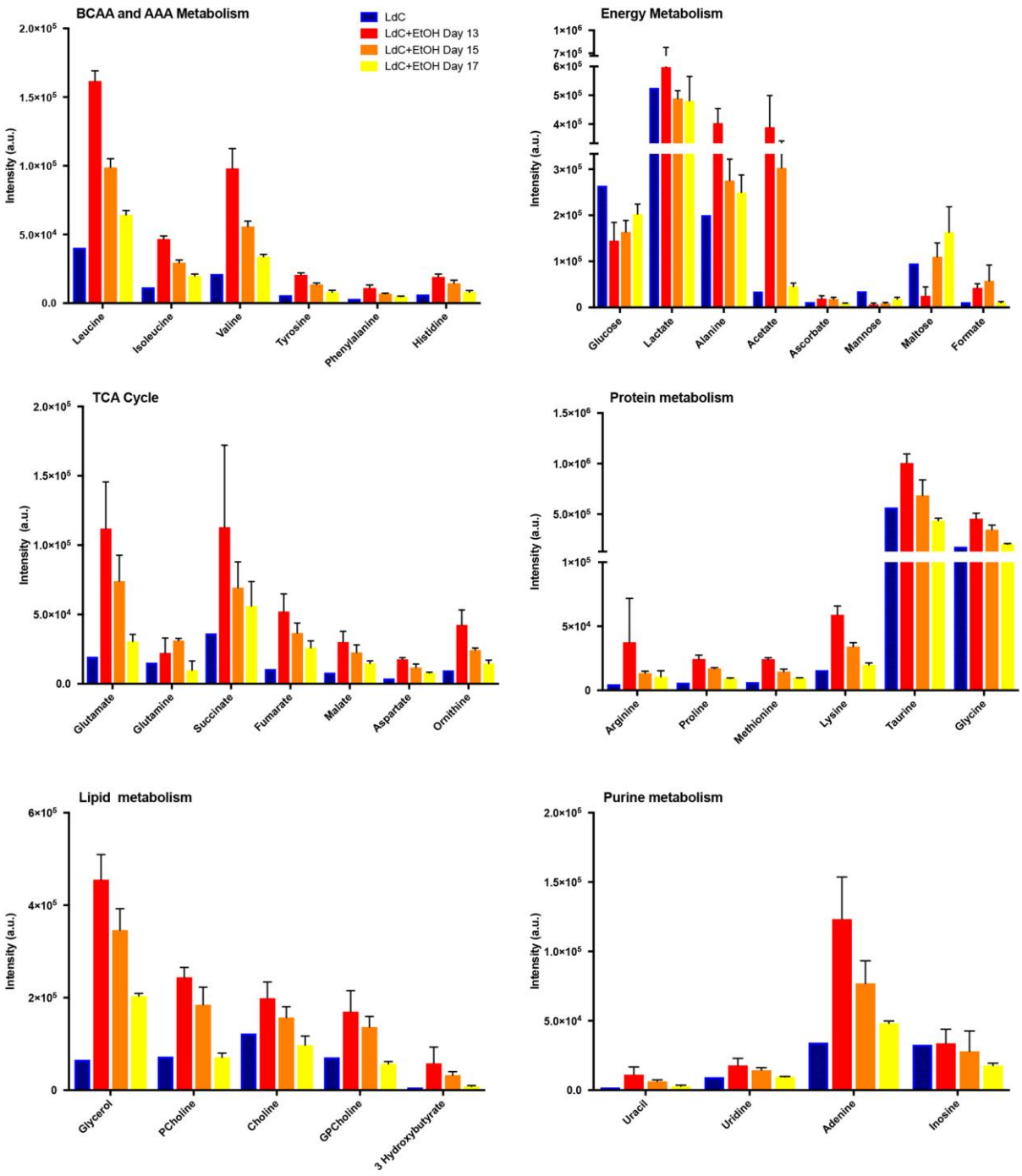

Figure 5: Exposure to ethanol-containing diet induces a transient change in hepatocyte energy metabolism. Polar metabolites were extracted from frozen liver lobes from animals exposed to LdC diet alone at day 17 (LdC) or LdC diet plus ethanol at days 13, 15 and 17. Data are averages of multiple samples prepared from single animals in the control groups and 3-4 animals on alcohol diets. All spectra were acquired at 300 K on a Bruker 600 MHz spectrometer with a TCI 1.7mm z-PFG cryogenic probe using a cooled Bruker SampleJet autosampler. 1D ^{1}H NMR spectra were processed using the NMRlab and Metabolab programmes within Matlab, version R2016b (MathWorks, Massachusetts, USA). Resonances were assigned using Chenomx (Alberta, Canada, 2015). Assigned peaks were then integrated in all spectra and metabolite intensities were compared between mice exposed to diet alone and LdC diet plus ethanol exposed samples on indicated days. Data are mean ± SEM of the group and have been divided into indicated categories of metabolites. Effects of diet were compared using two-way ANOVA which confirmed that for

all classes of metabolite there was a significant effect of diet on intensity of signal ($p<0.001$ for all metabolites). Tukey's multiple comparison test to compared individual diets. Here for all classes of metabolite control LdC was significantly different than day 13 and day15 timepoints on LdC plus ethanol. All metabolites except for BCAA and AAA metabolism were not significantly different in LdC and LdC plus EtOH at day 17 (for BCAA and AAA $p<0.001$ LdC vs LdC+EtOH at day 17).

Tables

Table 1 : Constituents of ad libitum alcohol diet administered to experimental animals

Ethanol % in the diet (vol/vol)	Dry mix (g)	Maltose dextrin (g)	Water (ml)	95% ethanol (ml)	Calories from maltose dextrin (%)	Calories from ethanol (%)
0	133	91.3	900	0	35.5	0
2.1%	133	62.9	910	21.1	24	11.5
4.2%	133	34.5	920	42.2	12.5	23
6.3%	133	6.1	930	63.3	1	34.5

Table 2: Antibodies used for flow cytometry

Antibody	Clone	Source and catalogue number	Fluorochrome	Stock Conc	Final Dilution
Lymphoid Master Mix					
CD49b	DX5	Biolegend 108913	FITC	0.5mg/ml	1:200
CD19	ID3	E-bioscience 25-0193-82	PE-Cy7	0.2mg/ml	1:100
CD8A	53-6.7	E-bioscience 45-0081-80	PERCYP5.5	0.2mg/ml	1:100
CD4	GK1.5	E-bioscience 17-0041-81	APC	0.2mg/ml	1:100
CD3	17A2	E-bioscience 558214	E450	0.2mg/ml	5:200
CD45	30-F11	E bioscience 563891	BV510	0.2mg/ml	1:50
Myeloid Master Mix					
Ly6C	HK1.4	E-bioscience 12-5932-82	PE	0.2mg/ml	1:600
Ly6G	1a8-Ly6G	E bioscience 17966882	APC	0.5mg/ml	1:300
CD45	30-F11	Biolegend 103132	PERCYP5.5	0.2mg/ml	1:200
CD11b	M1/70	E-bioscience 11-0112-82	FITC	0.5mg/ml	1:100
CD3	17A2	E-bioscience 558214	E450	0.2mg/ml	5:200
F4/80	Bm8	E-bioscience 25-4801-82	PE-Cy7	0.2mg/ml	1:50

Table 3 : Antibodies used for immunochemistry

Primary antibody	Secondary Antibody	Isotype control
Anti-Ly6G (e-bioscience rat anti-mouse ab 0.5mg/ml (clone RB6-8C5) used at 1:500 dilution)	ImmPRESS peroxidase anti-rat kit (Vector Labs)	Rat IgG2a (e-bioscience-eBR2a used at 1:500)
Anti-F4/80 rat anti-mouse ab (E-biosciences 14-4801) 0.5mg/ml used at 1:200 dilution	ImmPRESS peroxidase anti-rat kit (Vector Labs)	Rat IgG2a (e-biosciences eBR2a used at 1:200)
Anti-Ki67 rabbit anti-mouse ab from Abcam (ab16667) clone SP6 used at 1:200 dilution	Horse anti-rabbit antibody from Vector Laboratories (BA1100)	BA1000 anti-rabbit IgG (H+L)
Anti-CK19 rat anti-mouse monoclonal ab from DSHB 100ug/ml used at 1:250 dilution	ImmPRESS peroxidase anti-rat	Rat IgG2a (e-biosciences eBR2a used at 1:250)

Supplemental Figure 1

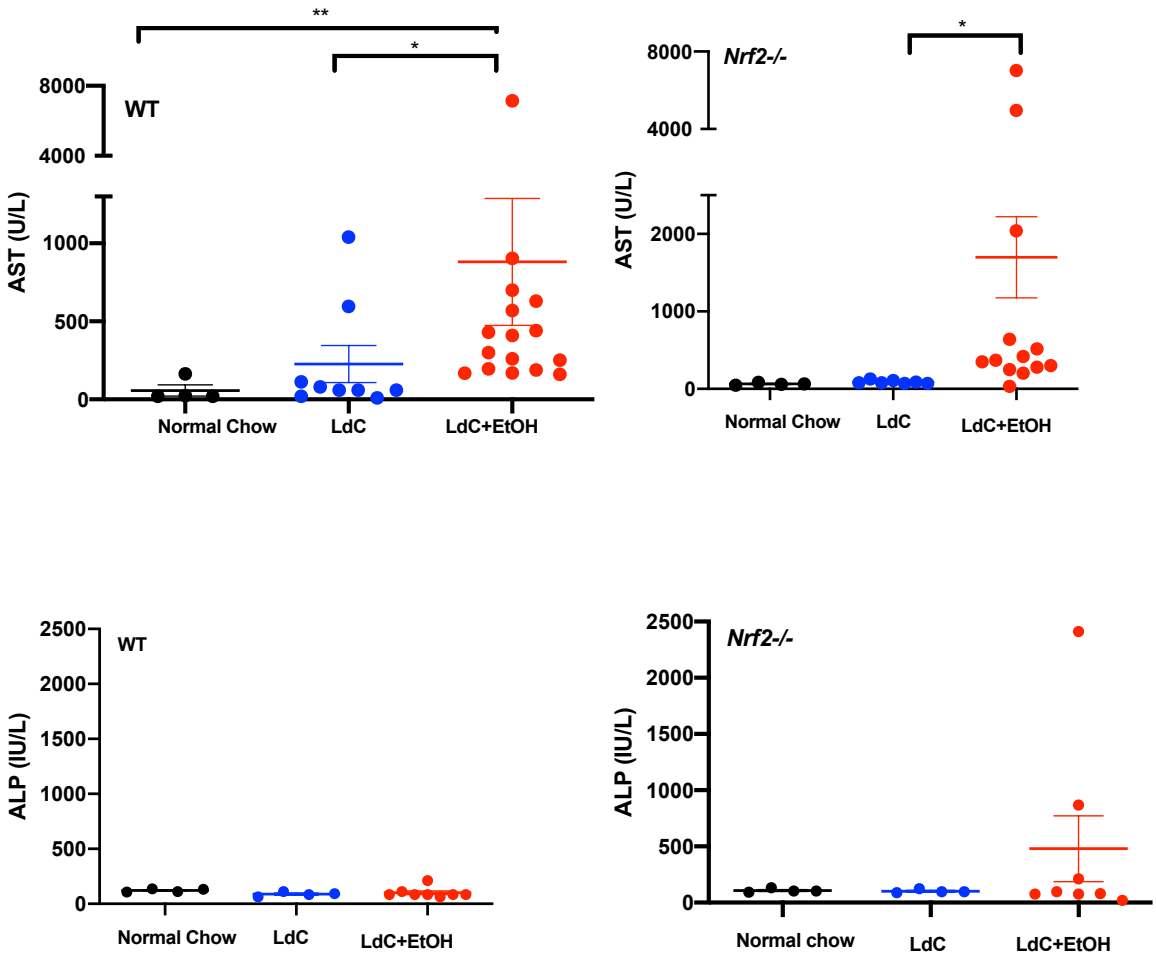

Figure S1 : Serum biochemical analysis from mice treated with modified LdC diet and ethanol WT and *Nrf2*$^{-/-}$ mice were fed LdC diet only for 5 days. At day 6 experimental groups received 2.2% EtOH mixed into the LdC diet. This was increased to 4.4% at day 9, and to 6.3% at day 12. Additionally, experimental groups received twice daily ethanol gavage of 33% EtOH (LdC+EtOH). Control mice received LdC diet only throughout the experiment and were not gavaged. Serum was prepared from WT and *Nrf2*$^{-/-}$ mice at day 15 for determination of ALST and AP concentration. Symbols are values from individual mice and bars are mean ±SEM for the group. Statistical difference level is indicated by * for $p<0.05$ and ** for $p<0.01$ performed with the Kruskal-Wallis Dunn's multiple comparison test.

Supplemental Figure 2

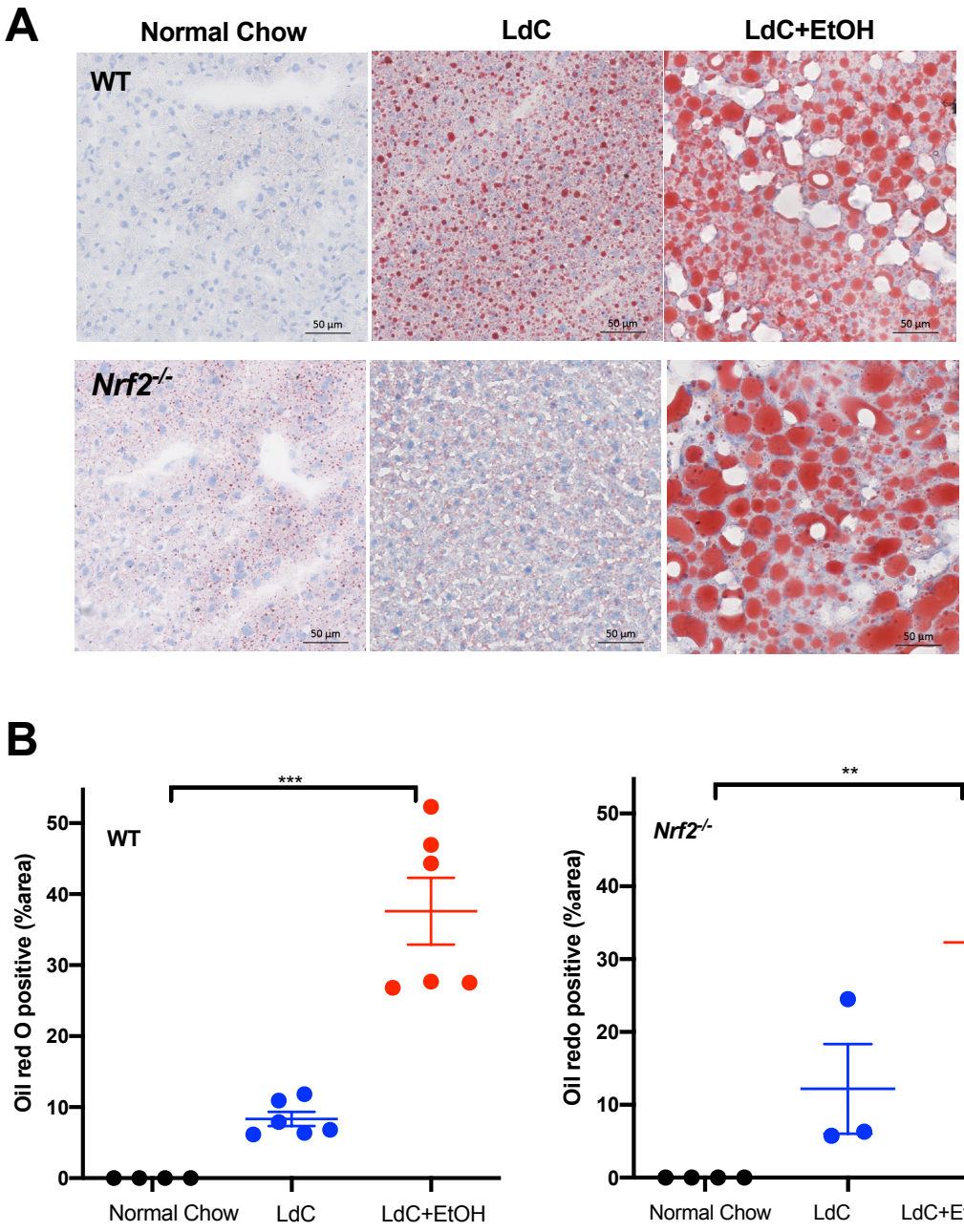

Figure S2: Mice fed ethanol-containing diet demonstrate significant liver steatosis. Accumulation of lipid droplets in hepatocytes within murine liver tissue sections was assessed by Oil red O staining. (A) Representative Oil Red O-stained liver sections from WT and *Nrf2*$^{-/-}$ mice fed normal chow, LdC or LdC+EtOH are shown. Scale bar is 50µm, data is representative of at least n=4 animals per group. (B) Quantification of extent of Oil Red O staining. Data form multiple fields of view per animal were captured using ImageJ and are expressed as a percentage of surface area occupied by lipid. Symbols are values from individual mice and bars represent mean ±SEM of the group. Statistical difference level is indicated by ** for $p<0.01$ or ***$p<0.001$ based on Kruskal-Wallis Dunn's multiple comparison test.

Supplemental Figure 3

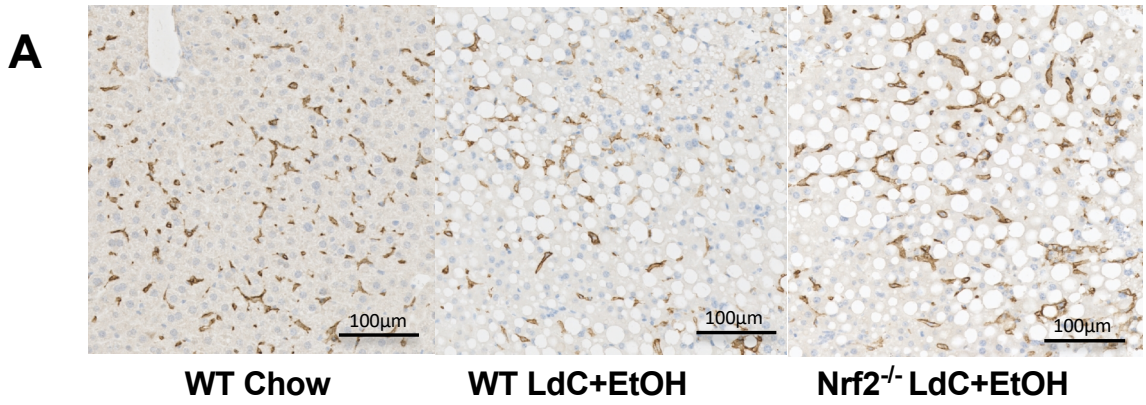

Figure S3: Staining for F4/80 positive cells suggests no change in number after exposure to ethanol. A : Representative images of F4/80+ cells in liver sections from WT and *Nrf2*$^{-/-}$ mice fed chow or LdC+EtOH as indicated, representative of at least n=3 animals per group. (B and C) Quantification of extent of F480 or Ly6G staining. Data from multiple fields of view per animal were captured using ImageJ and are expressed as a percentage of surface area occupied by F4/80 staining or number of Ly6G positive cells per field.Symbols are mean values from individual mice and bars represent mean ±SD of the group. Statistical difference level is indicated by ** for $p<0.01$ based on Kruskal-Wallis Dunn's multiple comparison test.

Figure S4: Staining for Ki67 positive cells 2 days after withdrawal of ethanol ethanol. Representative images from three individual animals where livers were harvested at day 17. Scale bar represents 100um and brown stained Ki67+ cells are distributed across the parenchyma in all cases.